HHS Public Access

Author manuscript

*Lasers Surg Med*. Author manuscript; available in PMC 2019 August 14.

Published in final edited form as:

*Lasers Surg Med*. 2018 July ; 50(5): 566–575. doi:10.1002/lsm.22824.

# Synthesis and In Vitro PDT Evaluation of New Porphyrins Containing *Meso*-Epoxymethylaryl Cationic Groups

**Jaqueline Carneiro**[1], **Alan Gonçalves**[1], **Zehua Zhou**[2], **Kaitlin E. Griffin**[2], **Nichole E.M. Kaufman**[2], **Maria da Graça Henriques Vicente**[2,*]

[1]Department of Pharmaceutical Sciences, Federal University of Paraná, Curitiba, Brazil

[2]Department of Chemistry, Louisiana State University, Baton Rouge, Louisiana

## Abstract

**Objectives:** Photodynamic therapy (PDT) is an effective cancer treatment that uses photosensitizers, light, and oxygen to destroy malignant cells. Porphyrins, and in particular the cationic derivatives, are the most investigated photosensitizers for PDT. In this context, it is important to study new methodologies to develop efficient cationic photosensitizers for use in PDT.

**Materials and Methods:** New porphyrins bearing cationic epoxymethylaryl groups were synthesized and characterized. Their cellular uptake, intracellular localization, and phototoxicity were evaluated in human HEp2 cells, and compared with their methylated analogs.

**Results:** All cationic porphyrins were efficient generators of singlet oxygen, with *quantum* yields in the range 0.35–0.61. The two methylated derivatives (3 and 4) accumulated the most within cells at all times investigated, up to 24 hours. Of these two porphyrins, 4 was the most phototoxic to the cells ($LD_{50}$ = 2.4 μM at 1.5 J/cm$^2$); however, porphyrin 3 also showed high phototoxicity ($LD_{50}$ = 7.4 μM at 1.5 J/cm$^2$). The epoxymethyl-containing porphyrins were found to be less phototoxic than the methylated derivatives, with $LD_{50}$>38 μM. The neutral porphyrins showed no phototoxicity up to the 100 μM concentrations investigated, and had the lowest singlet oxygen *quantum* yields. All cationic porphyrins localized mainly in the cell ER, Golgi apparatus, and lysosomes.

**Conclusion:** Our results suggest that cationic methylated porphyrin derivatives are promising PDT photosensitizing agents. The epoxymethyl-containing derivatives showed increased efficacy relative to the neutral analogs, and are good candidates for further investigation. Lasers Surg. Med. 50:566–575, 2018.

*Correspondence to: Maria da Graça Henriques Vicente, PhD, Department of Pharmaceutical Sciences, Federal University of Paraná, Curitiba, Brazil. vicente@lsu.edu.

This article is dedicated to Professor Thomas Dougherty.

Conflict of Interest Disclosures: All authors have completed and submitted the ICMJE Form for Disclosure of Potential Conflicts of Interest and none were reported.

SUPPORTING INFORMATION

Additional supporting information may be found in the online version of this article.

**Keywords**

porphyrin; PDT; epoxymethyl; cationic; cytotoxicity; cellular uptake

## INTRODUCTION

Photodynamic Therapy (PDT) has several advantages over other cancer treatments, such as surgery and radiation therapy, because it is relatively non-invasive; PDT is also considered to be a localized form of therapy due to the tendency of the photosensitizers to accumulate in cancer tissues, combined with controlled light delivery at a specific wavelength. The photosensitizer-accumulated malignant cells are then destroyed via necrosis and/or apoptosis due the action of singlet oxygen, and other reactive oxygen species (ROS) produced [1,2].

The most used photosensitizers in PDT are porphyrins and related compounds [3]. Porphyrins bearing positively charged groups have proven to be superior photosensitizers due to their interaction with specific cell structures, including with anionic DNA and RNA [4–6]. Porphyrins bearing a variable number and type of cationic groups have been successfully tested against cancer cells [5,7], keratinocytes [8], and microorganisms [9,10]. As was recently demonstrated by Slomp et al. [8], another benefit provided by cationic porphyrins relates to their superior capacity for production of singlet oxygen in comparison with their negatively charged or neutral analogs.

Quaternary nitrogen-containing porphyrins, particularly those bearing different combinations of *N*-methylated aminophenyl and pyridyl groups attached to the *meso* positions, are by far the most explored examples of cationic photosensitizers [5]. The literature shows that distinct cationic structures have improved PDI (Photodynamic Inactivation) [11,12] or PDT efficacy; for example, the successful replacement of a methyl group attached to the pyridyl nitrogen with long-chain alkyl groups [10,13] induces increased efficacy. Furthermore, the presence of phenyl groups interleaved with the *N*-methylpyridyl groups can result in porphyrins tending to form aggregates, which hinders their photosensitizing properties. In this way, the search for alternative *N*-alkylation methodologies that produce cationic porphyrin structures with different meso groups can be an important tool for the development of efficient photosensitizers.

In the present study, we have synthesized and examined the phototoxicity of new cationic porphyrins. Specifically, the porphyrins herein evaluated possess two distinct structural features of interest: the presence of (a) *meso*-dimethoxyphenyl instead of *meso*-phenyl groups as a non-cationic appendage and (b) cationic nitrogens displaying the epoxymethyl group. The former structural feature should prevent porphyrin aggregation behavior, while the later could permit conjugation of porphyrins with specific biological ligands, such as peptides, proteins, and carbohydrates [14,15].

# MATERIALS AND METHODS

## Chemistry

**General.—**Reagents and solvents were obtained from Sigma–Aldrich (St. Louis, MO) and VWR International. Reactions were monitored by TLC using 0.2 mm silica plates. For purification, column chromatography was performed using Sorbent Technologies 60 Å silica gel (230–400 mesh) and preparative thin layer chromatography was performed using Merck TLC silica gel 60 glass plates. The $^{1}$H NMR and $^{13}$C NMR spectra were obtained with a Bruker AV-400 spectrometer (400 MHz for $^{1}$H, 100 MHz for $^{13}$C) with the indicated solvents, and using TMS or residual solvent peaks as internal standards. Chemical shifts (d) are expressed in parts per million (ppm) and coupling constants (J) in Hertz (Hz). Mass spectra were obtained using an Agilent Technologies 6210 ESI-TOF. UV-Vis spectra were measured using an Agilent Cary50 spectrometer using porphyrin concentrations of $1.2 \times 10^{-5}$ mol $L^{-1}$ in $CH_2Cl_2$ or DMSO. Fluorescence emission spectra were collected using a Perkin Elmer LS-55 spectrometer using porphyrin concentrations of $2 \times 10^{-6}$ mol $L^{-1}$ in DMSO. Melting points were obtained using a Barnstead Mel-Temp Electrothermal Model 1001 Capillary Melting Point Apparatus.

**Synthesis of 5,10,15-tri(3,5-dimethoxyphenyl)-20-(4-pyridyl) porphyrin (1).—** Porphyrin **1** was synthesized according to a methodology previously described [3] with modifications. Pyrrole (780 μl, 12 mmol), 4-pyridinecarboxaldehyde (280 μl, 3 mmol), and 3,5-dimethoxybenzaldehyde (1.245 g, 9 mmol) were dissolved in 25 ml of propionic acid and maintained in reflux for 3 hours. After this period, 25 ml of acetone were added and the mixture filtered. Purification using silica gel column chromatography with chloroform/methanol 98:2 for elution gave 25.0% yield of the title porphyrin. MP =>300°C. **$^{1}$H NMR** (400 MHz, $CDCl_3$) δ 8.95 (d, *J* = 5.14 Hz, 2H), 8.91 (d, *J* = 4.65 Hz, 2H), 8.87 (s, 4H), 8.70 (d, *J* = 4.65 Hz, 2H), 8.08 (d, *J* = 5.31 Hz, 2H), 7.31 (d,*J* = 1.99 Hz, 6H), 6.82 (s, 3H), 3.88 (s, 18H), −2.92 (s, 2H).**$^{13}$C NMR** (100 MHz, $CDCl_3$) δ 159.1, 150.6, 148.5, 144.0, 129.7, 120.7, 120.4, 116.5, 114.1, 100.3, 55.9, 31.3. UV-Vis ($CH_2Cl_2$) $\lambda_{max}$ (log ε) 420 (4.83), 513 (3.44), 549 (2.96), 588 (3.14), 644 (2.88) nm. MS (ESI) *m/z* calc. for $[M + H]^+$, $C_{49}H_{41}N_5O_6^+$: 796.3129; Found: $[M + H]^+$: 796.3116.

**Synthesis of 5-(4-dimethylaminophenyl)-10,15,20-triphenylporphyrin (2).—** Porphyrin 2 was synthesized as previously reported [16]. Briefly, pyrrole (173 μl, 2.49 mmol), 4-(dimethylamino)benzaldehyde (93 mg, 0.62 mmol) and benzaldehyde (190 μl, 1.90 mmol) were dissolved in 250 ml of dichloromethane, then trifluoroacetic acid (963 μl) was added, and the solution was stirred for 20 min at room temperature. *p*-Chloranil (490 mg) was added and the mixture was maintained at 45°C for 1 hour. Triethylamine (1.74 ml) was then added and the solution was concentrated. Purification using silica column chromatography with dichloromethane/hexane 2:1 for elution gave the title porphyrin in 42.3% yield. The spectroscopic data were in agreement with the previous literature [16,17].

**Synthesis of 5-(1-methylpyridinium-4-yl)-10,15,20-tri(3,5-dimethoxyphenyl) porphyrin (3) and 5-(N,N, N-trimethyl-4-ammoniumphenyl)-10,15,20-triphenyl porphyrin (4).—**Methylation was performed following the literature, with some

modifications [18]. 20 mg of porphyrin 1 (0.025 mmol) or 2 (0.03 mmol) and methyl iodide (1 ml, 16 mmol) were added to 5 ml of DMF. The reaction was stirred for 5 hours at 45°C. Dichloromethane (25 ml) was added and the organic solution was washed with water and brine. The organic layer was dried over $Na_2SO_4$ and evaporated. Purification by recrystallization using $CH_2Cl_2/Et_2O$ gave 91% yield for 3 and 86% yield for 4. Data for porphyrin 4 is in agreement with literature [5,18]. Data for 3: MP = >300°C. $^1$**H NMR** (400 MHz, $DMSO_d$) δ 9.44 (d, *J* = 6.68 Hz, 2H), 9.05 (d, *J* = 4.60 Hz, 2H), 8.98 (m, 8H), 7.38 (d, *J* = 2.21 Hz, 6H), 7.02 (dd, *J* = 2.20 Hz, $J_1$ = 4.62 Hz, 3H), 4.70 (2, 3H), 3.94 (s, 18H), −2.96 (s, 2H) $^{13}$**C NMR** (100 MHz, $DMSO_d$) δ 158.7, 157.5, 143.9, 142.7, 132.2, 121.1, 120.45, 113.6, 113.0, 100.0, 55.5, 47.7, 30.6, 29.7. UV-Vis (DMSO) $\lambda_{max}$ (log ε) 425 (4.98), 516 (3.77), 553 (3.35), 589 (3.39), 645 (3.19) nm. MS (ESI) *m/z* calc. for $[M]^+$, $C_{50}H_{44}N_5O_6$: 810.3280; Found: $[M]^+$: 810.3293.

**Synthesis of 5-(1-epoxymethylpyridinium-4-yl)-10,15,20-tri(3,5-dimethoxyphenyl) porphyrin (5) and 5-(N-dimethylepoxymethyl-4-aminiumphenyl)-10,15,20-triphenyl porphyrin (6).—**Alkylation was performed by adding 20 mg of porphyrin 1 (0.025 mmol) or 2 (0.03 mmol) and epibromohydrin (2 ml, 23.37 mmol) to 5 ml of acetone. The reaction was maintained under reflux for 8 hours. After drying under vacuum, the residue was purified by prep-TLC plates using the solvent system chloroform/methanol/water (6:4:1). The yield obtained was 17% for 5 and 9% for 6. Data for 5: MP = >3008C. $^1$**H NMR**(400 MHz, $DMSO_d$) δ 9.45 (d, *J* = 6.21 Hz, 2H), 9.04–8.95 (m, 10H), 7.38 (d, *J* = 1.94 Hz, 6H), 7.01 (m, 3H), 6.45 (d,*J* = 4.35 Hz, 1H), 5.20 (d, *J* = 12.57 Hz, 1H), 4.84 (m, 1H), 4.55 (s, 1H), 3.93 (s, 18H), 3.82(dd, *J* = 6.03 Hz, $J_1$ =10.46 Hz, 1H), −2.96 (s, 2H). $^{13}$**C NMR** (100 MHz, DMSO) δ 158.9, 148.8, 142.7, 132.2, 120.4, 113.6, 112.8, 100.0, 72.4, 70.8, 63.3, 63.0, 62.7, 59.5, 55.4, 37.1, 28.8. UV-Vis (DMSO) $\lambda_{max}$ (log ε) 424 (4.73), 516 (3.54), 555 (3.21), 589 (3.25), 644 (3.07) nm. MS (ESI) *m/z* calc. for $[M]^+$, $C_{52}H_{46}N_5O_7$:852.3386; Found: $[M]^+$: 852.3392. Data for 6: MP = >300°-C. $^1$**H NMR** (400 MHz, $DMSO_d$) δ 8.84 (m, 8H), 8.51 (d, *J* = 8.82 Hz, 2H), 8.42 (d, *J* = 8.82 Hz, 2H), 8.22 (d, *J* = 6.71Hz, 6H), 7.84 (m, 9H), 5.13 (m, 1H), 4.71 (s, 1H), 4.14 (s, 1H), 3.92 (s, 6H), 3.62 (m, 2H), −2.92 (s, 2H). $^{13}$**C NMR** (100 MHz, DMSO) δ 206.4, 141.1, 135.3, 134.3, 127.1, 120.3, 70.9, 63.4, 56.7, 37.2, 31.2, 30.62, 28.9. UV-Vis (DMSO) $\lambda_{max}$ (log ε) 420 (5.05), 515 (3.68), 549 (3.39), 590 (3.30), 650 (3.40) nm. MS (ESI) *m/z* calc. for $[M]^+$,$C_{49}H_{40}N_5O$: 714.3221; Found: $[M]^+$: 714.3214.

## Cellular studies

**General.—**The human carcinoma HEp2 cells used in these studies were purchased from ATCC. The culture medium and other reagents were purchased from Life Technologies (Carlsbad, CA). The HEp2 cells were cultured in medium (DMEM:Advanced 1:1) containing 10% FBS and 1% antibiotic (penicillin-streptomycin). 32 mM porphyrin stock solutions were prepared by dissolving each porphyrin in 95% DMSO and 5% Cremophor EL (as a non-ionic emulsifier). The working concentrations were obtained by diluting the stock solution with growing medium.

**Time-dependent cellular uptake.—**The HEp2 cells were plated at 15,000 cells per well in a Costar 96-well plate (BD biosciences) and grown overnight. The cells were treated by

adding 100 μl/well of 10 μM working solution at different time periods of 0, 1, 2, 4, 8, and 24 hours. The loading medium was removed at the end of each treatment. The cells were washed with 1X PBS, and solubilized by adding 0.25% Triton X–100 in 1X PBS. A compound standard curve using 10, 5, 2.5, 1.25, 0.625, and 0.3125 μM concentrations was obtained by diluting the stock solution with 0.25% Triton X–100 (Sigma–Aldrich) in 1X PBS. A cell standard curve was obtained using 10,000, 20,000, 40,000, 60,000, 80,000, and 10,0000 cells per well. The cells were quantified using the CyQuant Cell Proliferation Assay (Life Technologies). The values were determined using a FluoStar Optima micro-plate reader (BMG LRBTEH), with wavelengths of 584/650 nm for the compounds and 485/520 nm for the cells. Cellular uptake is expressed in terms of pM/cell.

**Dark cytotoxicity.—**The HEp2 cells were placed in a 96-well plate as above, with the compound concentrations of 200, 100, 50, 25, 12.5, 6.25, and 0 μM (five repetitions for each concentration) and incubated at 37°C. After 24 hours incubation, the compound was removed by washing the cells with 1X PBS and replaced with medium containing 20% cell titer blue (CellTiter-Blue® assay, Promega, Madison, WI). The cells were incubated for an additional 4 hours at 37°C. A fluorescence-based assay was used for measuring the viable cells at 570/615 nm with a FluoStar Optima micro-plate reader. The dark toxicity is expressed in terms of the percentage of viable cells.

**Phototoxicity.—**Porphyrin concentrations of 100, 50, 25, 12.5, 6.25, 3.125, and 0 μM were used for the phototoxicity experiments. The HEp2 cells were placed in 96-well plates as described above, and treated with the compounds for 24 hours at 37°C. After 24 hours treatment, the loading medium was removed. The cells were washed once with 1X PBS, and then refilled with fresh medium. The cells were exposed to approximately 1.5 J/cm$^2$ light dose. After exposure to light, the cells were returned to the incubator for 24 hours. After this time, the medium was removed and replaced with medium containing 20% CellTiter-Blue®. The cells were incubated for an additional 4 hours. A fluorescence-based assay was used for measuring the viable cells at 570/615 nm with a FluoStar Optima microplate reader. The phototoxicity is expressed in terms of the percentage of viable cells.

**Microscopy.—**The subcellular localization of this series of compounds was investigated by fluorescence microscopy upon exposure of HEp2 cells to each compound at a concentration of 10 μM for 6 hours. The organelle trackers (Invitrogen, Carlsbad, CA) ER Tracker Blue/White (100 nM), BODIPY C5 Ceramide (50 nM), MitoTracker Green (250 nM), and LysoSensor Green (50 nM) were added to the cells half hour before imaging. The cells were washed three times with PBS solution and the images obtained using a Leica DM6B upright microscope equipped with a water immersion objective, and DAPI, GFP, and Texas Red filter cubes (Chroma Technologies, Bellows Falls, VT).

**Comparative singlet oxygen quantum yields.—**A standard solution of methylene blue (MB) was prepared at a concentration of 10 μM in DMSO. Each porphyrin was dissolved in DMSO at a concentration of 10 μM. To each well of a 6-well plate was added 3 ml each of DMSO, porphyrin solution, and MB solution. To each well was then added 3 ml of a 100 μM solution of DPBF in DMSO. The plate was irradiated with a light intensity of

1.25 mW/cm$^2$ for 1 hour, and UV-Vis absorption measurements were taken before irradiation ($t = 0$) and at 15, 30, 45, and 60 minutes after irradiation. UV/Vis absorbance's were plotted versus time points to obtain a fitted curve for the blank, standard and each sample. The slope of the curves was used to determine the *quantum* yield for each sample using the following equation:

$$\Phi_x = \Phi_{MB} \times S_x / S_{MB}$$

where Φ represents *quantum* yield, S represents the slope, and *x* and MB represent sample and methylene blue, respectively.

## RESULTS AND DISCUSSION

### Chemistry

Compound 1, bearing one *meso*-pyridyl group, was synthesized in 25% yield by cyclocondensation of pyrrole, 4-pyridinecarboxaldehyde, and 3,5-dimethoxybenzaldehyde, using Adler-Longo conditions with some modifications. The reaction was successful in terms of yield, compared with previously reported *meso*-pyridyl porphyrins [9,19,20]. This might be due to the enhanced solubility of porphyrin 1 compared with the *meso*-phenyl analogs, which facilitated its purification. Porphyrin 1 was then used as precursor for the alkylation reactions to give its cationic derivatives 3 and 5 (Scheme 1).

An attempt to synthesize compound 2 also using an Adler-Longo methodology was performed; however, the yields obtained in this case were very low (0.47%). Therefore, porphyrin 2 was synthesized by means of a one-pot, two-step methodology, as previously reported [16]. The purification step was accomplished by silica gel column chromatography using the solvent system dichloromethane/hexane 2:1, which resulted in a relatively high yield (42.3%) compared with that reported in the literature (19.5%) [16]. The spectroscopic characterization data for this porphyrin is in agreement with those previously reported [16,17]. After purification and characterization, compound 2 was used as starting material for the quaternization reactions (Scheme 2). Interestingly, porphyrin 2 showed significant lower fluorescence intensity compared with porphyrin 1 (see Supplemental Information).

The first cationic derivatives were synthesized *via* a methylation reaction using an excess of methyl iodide, in DMF, to give compounds 3 (91% yield) and 4 (86% yield). Methylation reactions with pyridylporphyrins were reported with yields varying between 27% and 90% [5,9,20–22]. Porphyrin 4, also previously reported, was obtained in 70% yield [5,18].

Each of the precursor porphyrins (1 and 2) were subjected to an alkylation reaction using epibromohydrin as the alkylating agent, to give compounds 5 (17% yield), and 6 (9% yield) as cationic derivatives. These compounds bear an epoxide group, which gives the porphyrin the potential capacity to subsequently link to other molecules [23–26].

## Cellular properties

The time-dependent uptake of porphyrins 1–6 was evaluated at a concentration of 10 μM over a period of 24 hours (Fig. 1). Porphyrins 3 and 4 were rapidly accumulated inside the HEp2 cells in the first 4 hours, with compound 4 being slightly faster to accumulate, and after that a plateau was reached. Compounds 3 and 4 correspond to the methylated derivatives of porphyrins 1 and 2, respectively, with the cationic derivatives accumulating four times more, at all time points investigated, in comparison with their synthetic precursors. Porphyrin 2 and its epoxide derivative 6 accumulate in cells slightly more than porphyrin 1 and its epoxide derivative 5. The following order of increasing uptake after 24 hours was determined: 3~4>>2>6~5>1. In general, as expected and previously reported [7,22,27], the accumulation values were higher for the cationic derivatives, which is probably due to the fact that cell membranes are negatively charged. It was also observed that the cationic derivatives bearing the epoxymethyl group accumulated poorly in comparison to the exclusively methylated porphyrins. This observation possibly reflects the differences in the way that these porphyrins interact with cell membranes. The alkylating properties of the epoxide group, present in porphyrins 5 and 6, could prevent their access to intracellular targets due to their potential immobilization in media structures, for example by reaction with proteins. It was previously reported that the epoxide group possesses the reactivity that enables the coupling with nucleophilic sites at the protein surface [28,29].

The subcellular sites of localization of the cationic porphyrins were investigated by fluorescence microscopy. Organelle-specific fluorophores BODIPY Ceramide (Golgi), LysoSensor Green (lysosomes), MitoTracker Green (mitochondria), and ER Tracker Blue/White (ER) were used in the overlay experiments. The purple or yellow/orange colors in Figures 2–5 indicate co-localization of porphyrin and organelle tracker, and the results are summarized in Table 1. All porphyrins localized mainly in the cell lysosomes, Golgi, and ER. In addition, porphyrins 4 and 6 were also found in mitochondria. All these organelles are important PDT targets that can lead to cell death upon light irradiation due to photodamage to anti-apoptotic Bcl-2 proteins and/or by direct organelle photodamage [30].

Porphyrins 1–6 were also evaluated in terms of their cytotoxicity against human carcinoma HEp2 cells using a Cell Titer Blue assay. This assay provides a simple, fast, sensitive and accurate method for determination of cell viability based on the generation of a fluorescente product (resazurin is reduced to resorufin), and it has been shown to correlate well with other methods for measuring cell proliferation and cytotoxicity. In order to detect any light-independent cytotoxicity, the dark toxicity was first assayed by examining cell toxicity after incubation with increasing concentrations of the porphyrins in the absence of light. Results shown in Figure 6 indicate low dark toxicities for all the porphyrins at concentrations up to 200 μM ($LD_{50}$> 200 μM). Cationic porphyrins previously reported exhibited $LD_{50}$ in the dark varying between 25–445 μM in various cell lines [5,27,31,32].

The phototoxicity assay (Fig. 7) was performed by exposing the HEp2 cells to approximately 1.5 J/$cm^2$ of light dose, after incubating the cells with the compounds at concentrations up to 100 μM. We determined the following order of decreasing phototoxicity: 4>3>6>5>2~1 (Table 2). It was noticed that epoxymethyl-containing compound 6, which did not shown an appreciable uptake value, displayed moderate

phototoxicty ($LD_{50}$ 38 μM). This result suggests that the extent of cellular uptake does not necessarily correlate with the observed phototoxicity, and that other factors, including the sites of intracellular localization, ability to produce ROS, and potential biomolecule targets, determine the cytotoxicity of the compounds.

The lack of a correlation between phototoxicity and the amount of porphyrin sequestered within the cells has been previously reported [5,33]. This is explained by the fact that the phototoxicity is highly dependent not only on the ability of the photosensitizer to accumulate within cells, but also on its intracellular targets and ability to generate ROS and/or $^1O_2$ upon light activation. The singlet oxygen *quantum* yields were determined in DMSO for this series of porphyrins (Table 2) by measuring the change in absorbance of 1,3-diphenylisobenzofuran (DPBF), as previously reported [34]. Our results show that the cationic porphyrins 3, 4, 5, and 6 are more efficient producers of singlet oxygen compared with the neutral derivatives 1 and 2. Among the cationic derivatives, 3, 4, and 5 were the most efficient singlet oxygen generators, with *quantum* yields in the range 0.52–0.61. These results are in agreement with previous reports showing that cationic porphyrins have the ability to generate $^1O_2$ [35–37]. In the present study porphyrins 3 and 4 showed the highest uptake, high singlet oxygen *quantum* yields, and also the highest phototoxicity. This suggests that the phototoxicity observed for these porphyrins is in part due to their high cellular uptake and to their ability to generate singlet oxygen. Compound 4 was found to be the most phototoxic with a $LD_{50}$ of 2.4 μM. Porphyrin 3 also showed high phototoxicity with a $LD_{50}$ of 7.4 μM. In agreement with this result, phototoxic cationic porphyrins are reported to have $LD_{50}$ values varying between 3–8 μM in human HEp2 cells with similar light dose [5,27]. On the other hand, the cationic porphyrins 5 and 6 bearing one epoxymethyl group, were found to be less phototoxic than their methylated derivatives, with $LD_{50}$ values of 100 and 38 μM, respectively, although they are still efficient singlet oxygen generators, particularly 5. This might be due to their much lower uptake into cells, as shown in Figure 1, and/or their reactivity toward nucleophiles. The neutral porphyrins 1 and 2 showed no phototoxicity up to the 100 μM concentration investigated, and displayed the lowest singlet oxygen *quantum* yields.

## CONCLUSIONS

A series of four cationic porphyrins bearing one *meso*-pyridyl or quaternary ammonium groups were synthesized and their biological properties in human HEp2 cells, were compared with their neutral derivatives. All porphyrins were non-toxic in the dark ($LD_{50}$ > 200 μM), and upon light irradiation, only the cationic derivatives were found to be phototoxic. Among these, the 5-(4-trimethylammoniumphenyl)-10,15,20-triphenylporphyrin 4 was the most phototoxic ($LD_{50}$ = 2.4 μM, 1.5 J/cm$^2$) followed by the 5-(4-methylpyridiniumphenyl)-10,15,20-tri(3,5-dimethoxyphenyl)porphyrin 3 ($LD_{50}$= 7.4 μM, 1.5 J/cm$^2$). The cationic porphyrins bearing one epoxymethyl group, 5 and 6, were less phototoxic than their methylated derivatives ($LD_{50}$ > 38 μM, 1.5 J/cm$^2$), in part due to their lower cellular uptake, potentially due to their higher reactivity compared with 3 and 4. The cationic porphyrins were found to be more efficient singlet oxygen producers compared with the neutral porphyrin derivatives, and localized mainly in the cell ER, Golgi and lysosomes. Among the series evaluated, porphyrins 3 and 4 are the most promising candidates for PDT

applications, while porphyrins 5 and 6 have potential capacity to bioconjugate to other molecules *via* the epoxymethyl group.

## Supplementary Material

Refer to Web version on PubMed Central for supplementary material.

## ACKNOWLEDGMENTS

This research was supported by the U. S. National Institutes of Health, grant number R01 CA179902. The authors are grateful to CAPES and CNPq (Brazil) for financial support to JC.

Contract grant sponsor: National Cancer Institute; Contract grant number: R01 CA179902.

## REFERENCES

1. Dougherty TJ, Gomer CJ, Henderson BW, et al. Photodynamic therapy. J Natl Cancer Inst 1998;90(12):889–805. [PubMed: 9637138]
2. Brown SB, Brown EA, Walker I. The present and future role of photodynamic therapy in cancer treatment. Oncology 2004; 5:497–408. [PubMed: 15288239]
3. Adler AI, Longo FL, Finarelli JD, et al. A simplified synthesis for *meso*-tetraphenylporphin. J Org Chem 1967;32(2):476.
4. McMillin DR, Shelton AH, Bejune SA, et al. Understanding binding interactions of cationic porphyrins with B-form DNA. Coord Chem Rev 2005;249:1451–1459.
5. Jensen TJ, Vicente MGH, Luguya R, et al. Effect of overall charge and charge distribution on cellular uptake, distribution and phototoxicity of cationic porphyrins in HEp2 cells. J Photochem Photobiol B 2010;100:100–111. [PubMed: 20558079]
6. Huang Z A Review of progress in clinical photodynamic therapy. Technol Cancer Res Treat 2005;4(3):283–293. [PubMed: 15896084]
7. Hao E, Jensen TJ, Vicente MGH. Synthesis of porphyrin-carbohydrate conjugates using “click” chemistry and their preliminary evaluation in human HEp2 cells. J Porphyrins Phthalocyanines 2009;13:51–59.
8. Slomp AM, Barreira SMW, Carrenho LZB, et al. Photodynamic effect of *meso*-(aryl)porphyrins and *meso*-(1-methyl-4-pyridinium)porphyrins on HaCaT keratinocytes. Bioorganic Med Chem Lett 2017;27:156–161.
9. Vandresen CC, Gonçalves AG, Ducatti DRB, et al. In vitro photodynamic inactivation of conidia of the phytopathogenic fungus *Colletotrichum graminicola* with cationic porphyrins. Photochem Photobiol Sci 2016;15:673–681. [PubMed: 27109559]
10. Reddi E, Ceccon M, Valduga G, et al. Photophysical properties and antibacterial activity of *meso*-substituted cationic porphyrins. Photochem Photobiol 2002;75(5):462–470. [PubMed: 12017471]
11. Malikt Z, Hanania J, Nitzan Y. New trends in photobiology (Invited Review) Bactericidal effects of photoactivated porphyrins—an alternative approach to antimicrobial drugs. J Photochem Photobiol B 1990;5:281–293. [PubMed: 2115912]
12. Müller A, Preub A, Röder B. Photodynamic inactivation of Escherichia coli—Correlation of singlet oxygen kinetics and phototoxicity. J Photochem Photobiol B 2018;178: 219–227. [PubMed: 29156350]
13. Stallivieri A, Guern FL, Vanderesse R, et al. Synthesis and photophysical properties of the photoactivatable cationic porphyrin 5-(4-Ndodecylpyridyl)-10,15,20-tri(4-N-methylpyridyl)-21H, 23H-porphyrin tetraiodide for anti-malaria PDT. Photochem Photobiol Sci 2015;14:1290–1295. [PubMed: 26066986]
14. Zheng X, Pandey RK. Porphyrin-carbohydrate conjugates: impact of carbohydrate moieties in photodynamic therapy (PDT). Anticancer Agents Med Chem 2008;8:241–268. [PubMed: 18393785]

15. Umezawa N, Matsumoto N, Iwama S, et al. Facile synthesis of peptide-porphyrin conjugates: towards artificial catalase. Bioorganic Med Chem 2010;18:6340–6350.
16. Ojadi ECA, Linschitz H, Gouterman M, et al. Sequential protonation of *meso*-*p*(dimethylamino)phenyl)porphyrins: charge-transfer excited states producing hyperporphyrins. J Phys Chem 1993;97:13192–13197.
17. Walter RI, Ojadi ECA, Linschitz H. A proton NMR study of the reactions with acid of *meso*-tetraphenylporphyrins with various numbers of 4-dimethylamino groups. J Phys Chem 1993;97:13308–13312.
18. Chen B, Wang WQP, Ma TTH, et al. Synthesis of β-substituted cationic porphyrins and their interactions with DNA. Bioorg Med Chem Lett 2003;13:3731–3733. [PubMed: 14552768]
19. Meng GG, James BR. Porphyrin chemistry pertaining to the design of anti-cancer drugs; part 1, the synthesis of porphyrins containing *meso*-pyridyl and *meso*-substituted phenyl functional groups. Can J Chem 1994;72:1894–1909.
20. Sun L, Chen H, Zhang Z, et al. Synthesis and cancer cell cytotoxicity of water-soluble gold(III) substituted tetraarylporphyrin. J Inorg Biochem 2012;108:47–52. [PubMed: 22265838]
21. Casas C, Saint-James B, Loup C, et al. Synthesis of cationic metalloporphyrin precursors related to the design of DNA cleavers. J Org Chem 1993;58(10):2913–2917.
22. Meng GG, James BR. Porphyrin chemistry pertaining to the design of anti-cancer drugs; part 2, the synthesis and in vitro tests of water-soluble porphyrins containing, in the meso positions, the functional groups: 4-methylpyridinium, or 4-sulfonatophenyl, in combination with phenyl, 4-pyridyl, 4-nitrophenyl, or 4-aminophenyl. Can J Chem 1994;72: 2447–2457.
23. Ferris DP, Lu J, Gothard C, et al. Synthesis of biomolecule-modified mesoporous silica nanoparticles for targeted hydrophobic drug delivery to cancer cells. Small 2011;7(13): 1816–1826. [PubMed: 21595023]
24. Lotz A, Heller M, Brieger J, et al. Derivatization of plasma polymerized thin films and attachment of biomolecules to influence HUVEC-Cell Adhesion. Plasma Process Polym 2012;9:10–16.
25. Janissen R, Oberbarnscheidt L, Oesterhelt F. Optimized straight forward procedure for covalent surface immobilization of different biomolecules for single molecule applications. Colloids Surf B 2009;71:200–207.
26. Kang DH, Jung H, Lee J, et al. Design of polydiacetylene-phospholipid supramolecules for enhanced stability and sensitivity. Langmuir 2012;28:7551–7556. [PubMed: 22515382]
27. Sibrian-Vazquez M, Hu X, Jensen TJ, Vicente MGH. Synthesis and cellular studies of PPIX-homing peptide conjugates. J Porphyrins Phthalocyanines 2012;16:603–615.
28. Chen G, Heim A, Riether D, et al. Reactivity of functional groups on the protein surface: development of epoxide probes for protein labeling. J Am Chem 2003;125:8130–8133.
29. Lee MH, Brass DA, Morris R, et al. The effect of non-specific interactions on cellular adhesion using model surfaces. Biomaterials 2005;26:1721–1730. [PubMed: 15576146]
30. Kessel D Correlation between subcellular localization and photodynamic efficacy. J Porphyrins Phthalocyanines 2004;8: 1009–1014.
31. Easson MW, Fronczek FR, Jensen T, Vicente MGH. Synthesis and in vitro properties of trimethylamine- and phosphonate-substituted carboranylporphyrins for application in BNCT. Bioorg Med Chem 2008;16(6):3191–3208. [PubMed: 18178445]
32. Sibrian-Vazquez M, Jensen TJ, Fronczek FR, et al. Synthesis and characterization of positively charged porphyrin-peptide conjugates. Bioconjugate Chem 2005;16:852–863.
33. Sibrian-Vazquez M, Jensen TJ, Vicente MGH. Porphyrinretinamides: synthesis and cellular studies. Bioconjugate Chem 2007;18:1185–1193.
34. Gibbs JH, Zhou Z, Kessel D, Fronczek FR, Pakhomova S, Vicente MGH. Synthesis, spectroscopic, and in vitro investigations of 2,6-diiodo-BODIPYs with PDT and multi-mode imaging applications. J Photochemistry Photobiology B Biol 2015;145:35–47.
35. Slomp AM, Barreira SMW, Carrenho LZB, et al. Photodynamic effect of *meso*-(aryl)porphyrins and *meso*-(1-methyl-4-pyridinium)porphyrins on HaCaT keratinocytes. Bioorganic Med Chem Lett 2017;27:156–161.

36. Vandresen CC, Gonçalves AG, Ducatti DRB, et al. In vitro photodynamic inactivation of conidia of the phytopathogenic fungus Colletotrichum graminicola with cationic porphyrins. Photochem Photobiol Sci 2016;15:673–681. [PubMed: 27109559]

37. Deda KD, Pavani C, Carita E, et al. Correlation of photodynamic activity and singlet oxygen quantum yields in two series of hydrophobic monocationic porphyrins. J Porphyrins Phthalocyanines 2012;16:55–63.

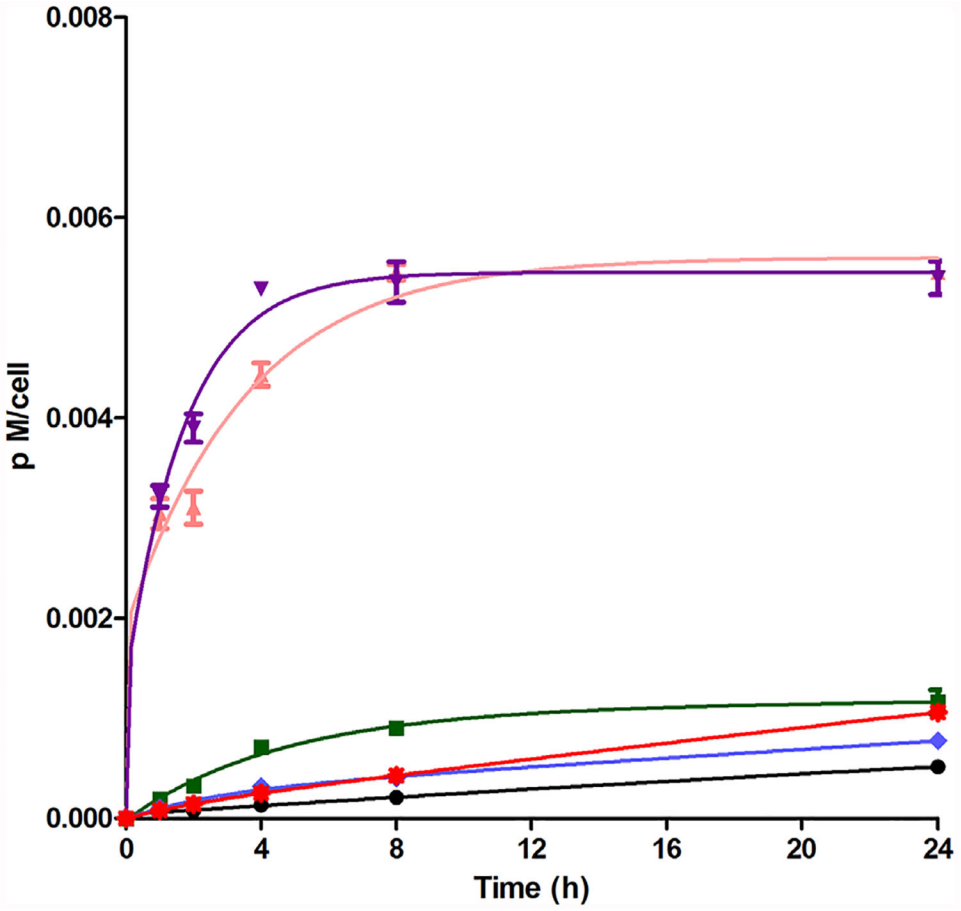


**Fig. 1.**

Time-dependent cellular uptake of porphyrins 1 (●), 2 (■), 3 (▲), 4 (▼), 5 (◆), and 6 (✸) at 10 μM by HEp2 cells.

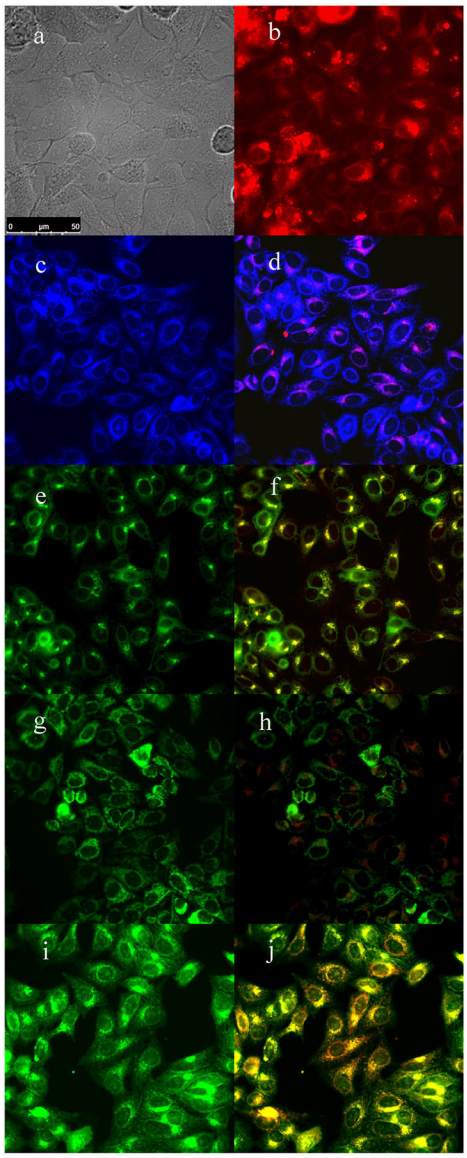


**Fig. 2.**

Subcellular localization of porphyrin 3 in HEp2 cells at 10 μM for 6 hours. (a) Phase contrast, (b) porphyrin 3, (c) ER Tracker Blue/White, (d) overlay of 3 and ER Tracker, (e) BODIPY Ceramide, (f) overlay of 3 and BODIPY Ceramide, (g) MitoTracker Green, (h) overlay of 3 and MitoTracker, (i) LysoSensor Green, and (j) overlay of 3 and LysoSensor Green. Scale bar: 10 μm.

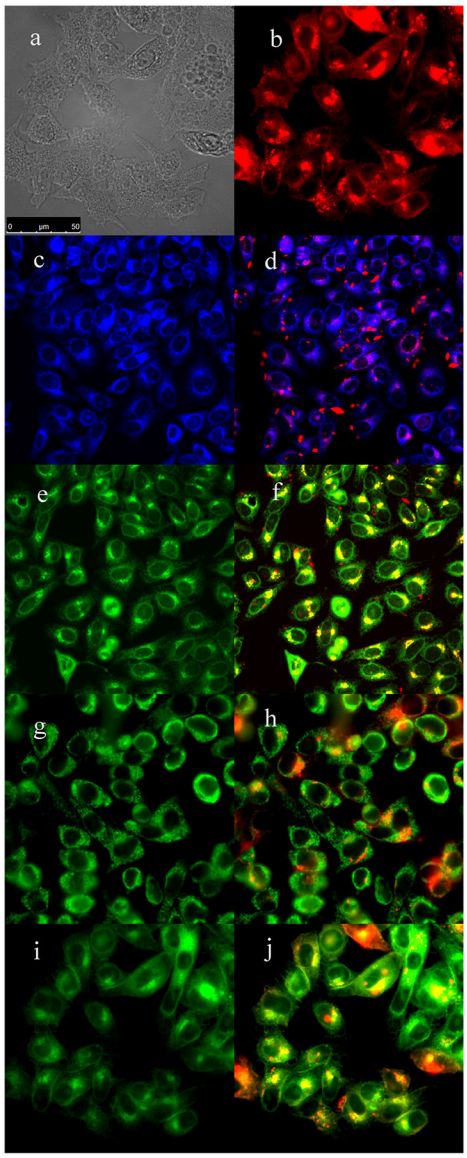


**Fig. 3.**

Subcellular localization of porphyrin 4 in HEp2 cells at 10 μM for 6 hours. (a) Phase contrast, (b) porphyrin 4, (c) ER Tracker Blue/White, (d) overlay of 4 and ER Tracker, (e) BODIPY Ceramide, (f) overlay of 4 and BODIPY Ceramide, (g) MitoTracker Green, (h) overlay of 4 and MitoTracker, (i) LysoSensor Green, and (j) overlay of 4 and LysoSensor Green. Scale bar: 10 μm.

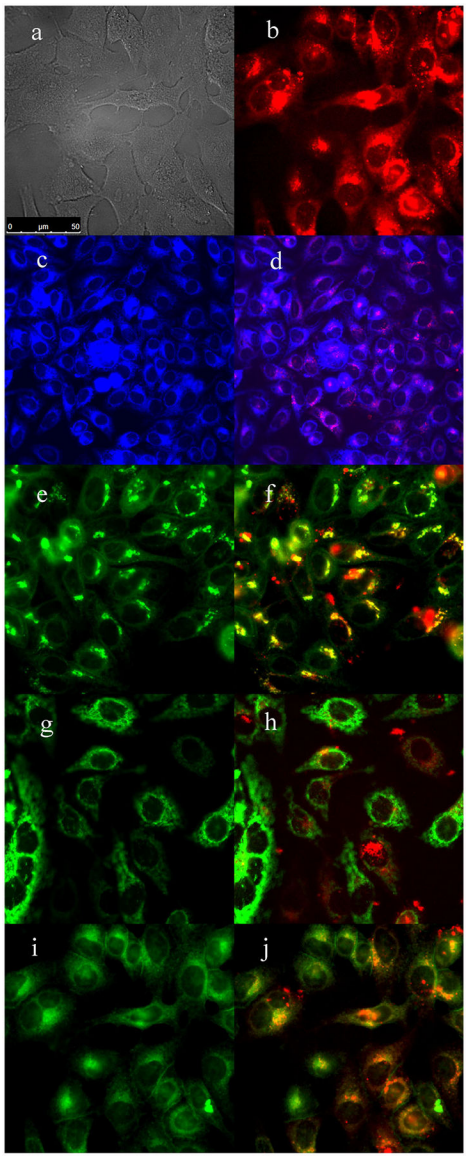


**Fig. 4.**

Subcellular localization of porphyrin 5 in HEp2 cells at 10 μM for 6 hours. (a) Phase contrast, (b) porphyrin 5, (c) ER Tracker Blue/White, (d) overlay of 5 and ER Tracker, (e) BODIPY Ceramide, (f) overlay of 5 and BODIPY Ceramide, (g) MitoTracker Green, (h) overlay of 5 and MitoTracker, (i) LysoSensor Green, and (j) overlay of 5 and LysoSensor Green. Scale bar: 10 μm.

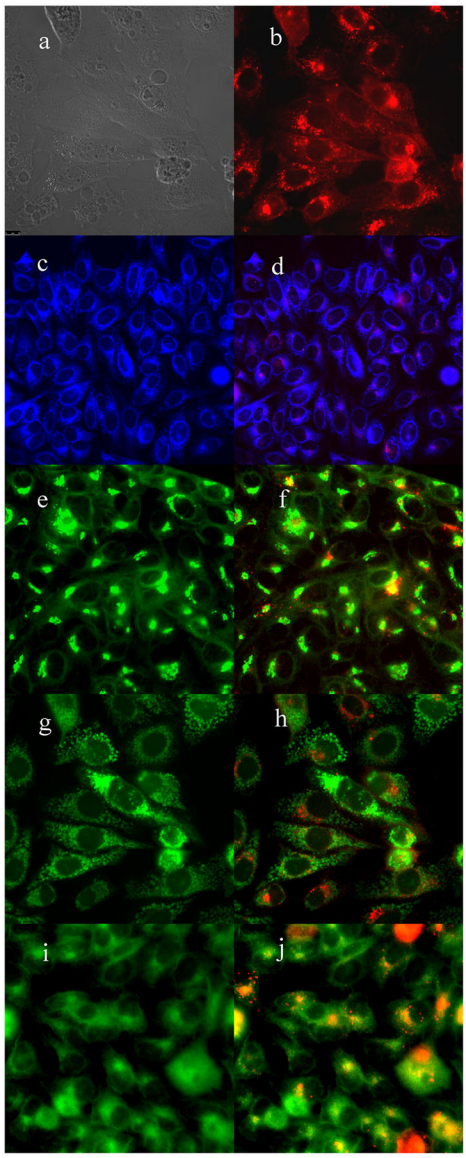


**Fig. 5.**

Subcellular localization of porphyrin 6 in HEp2 cells at 10 μM for 6 hours. (a) Phase contrast, (b) porphyrin 6, (c) ER Tracker Blue/White, (d) overlay of 6 and ER Tracker, (e) BODIPY Ceramide, (f) overlay of 6 and BODIPY Ceramide, (g) MitoTracker Green, (h) overlay of 6 and MitoTracker, (i) LysoSensor Green, and (j) overlay of 6 and LysoSensor Green. Scale bar: 10 μm.

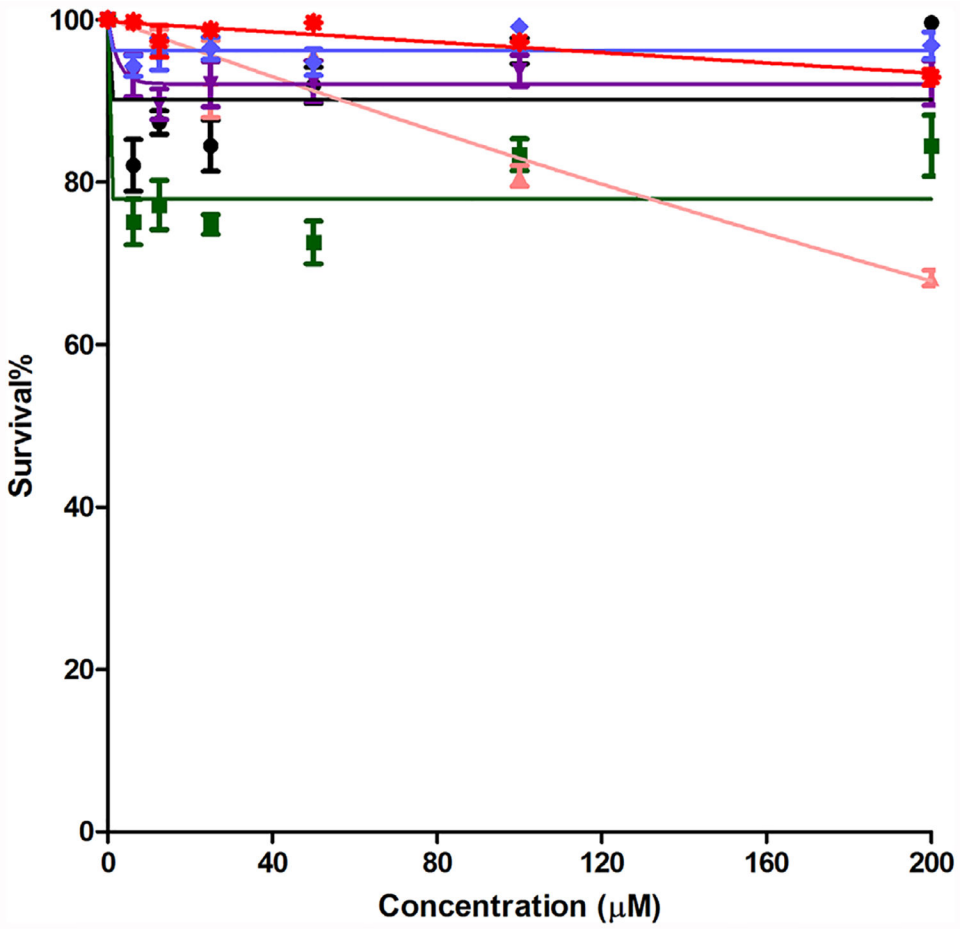


**Fig. 6.**

Darktoxicity of porphyrins 1 (●), 2 (■), 3 (▲), 4 (▼), 5 (◆), and 6 (✸) using HEp2 cells and a Cell Titer Blue assay.

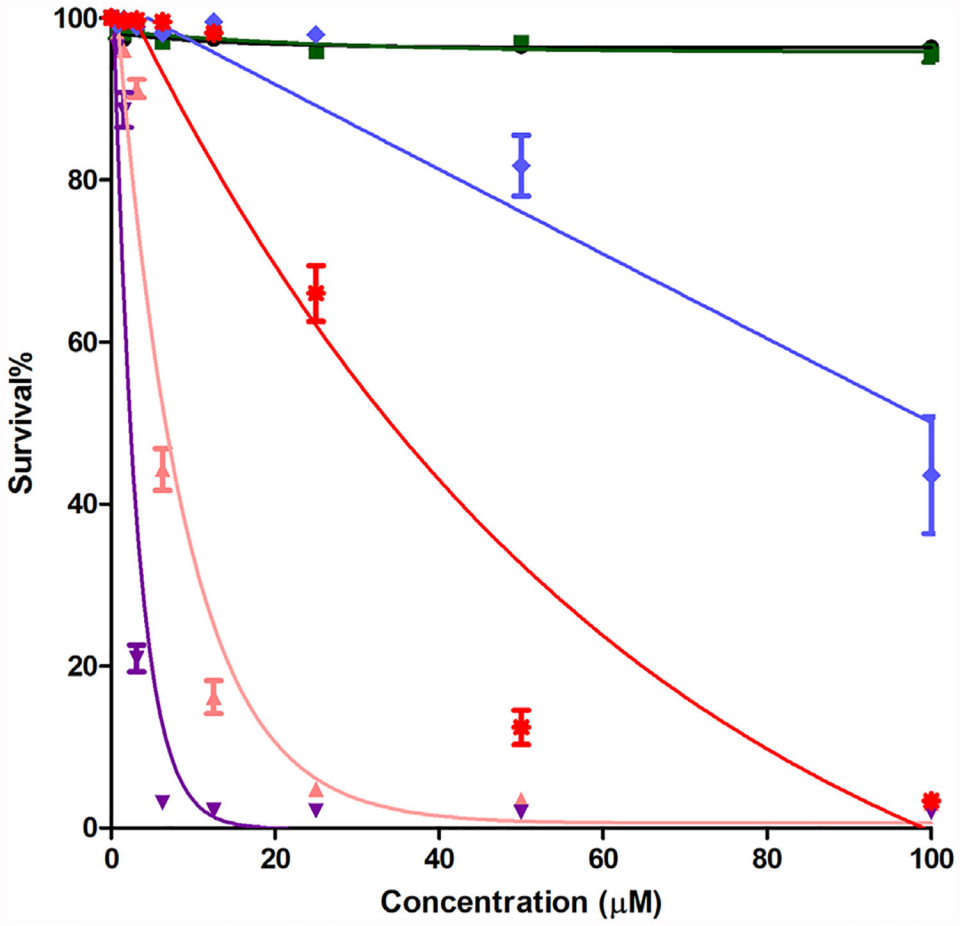


**Fig. 7.**

Phototoxicity (1.5 J/cm$^2$) of porphyrins 1 (●), 2 (■), 3 (▲), 4 (▼), 5 (◆), and 6 (✸) using HEp2 cells and a Cell Titer Blue assay.

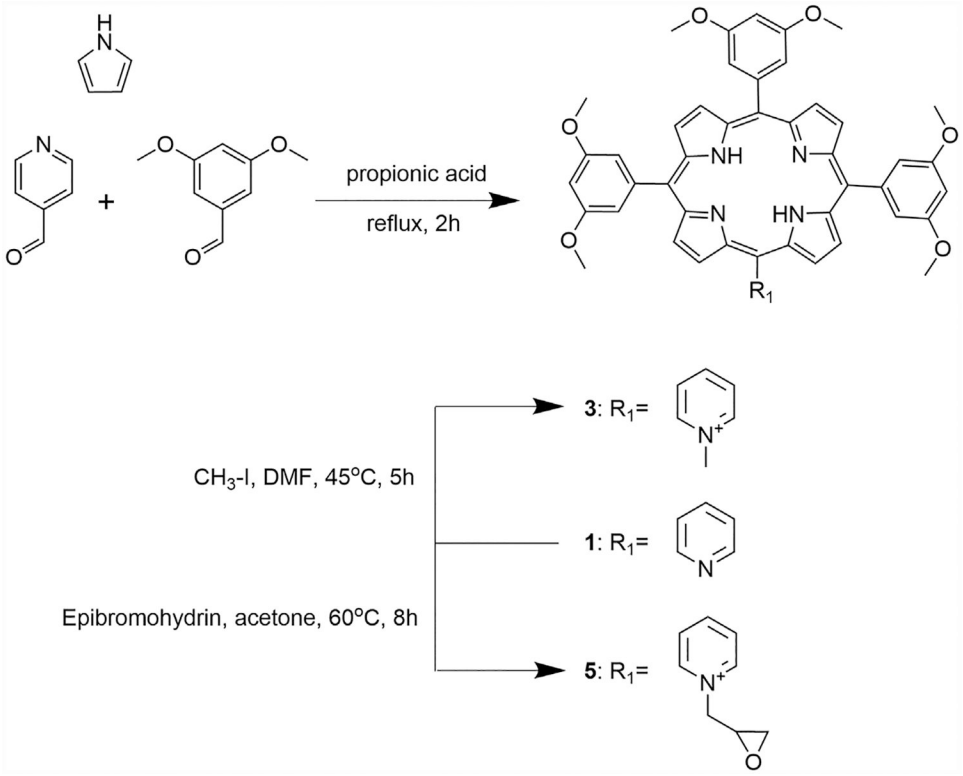


**Scheme 1.**
Synthesis of porphyrins 1, 3, and 5.

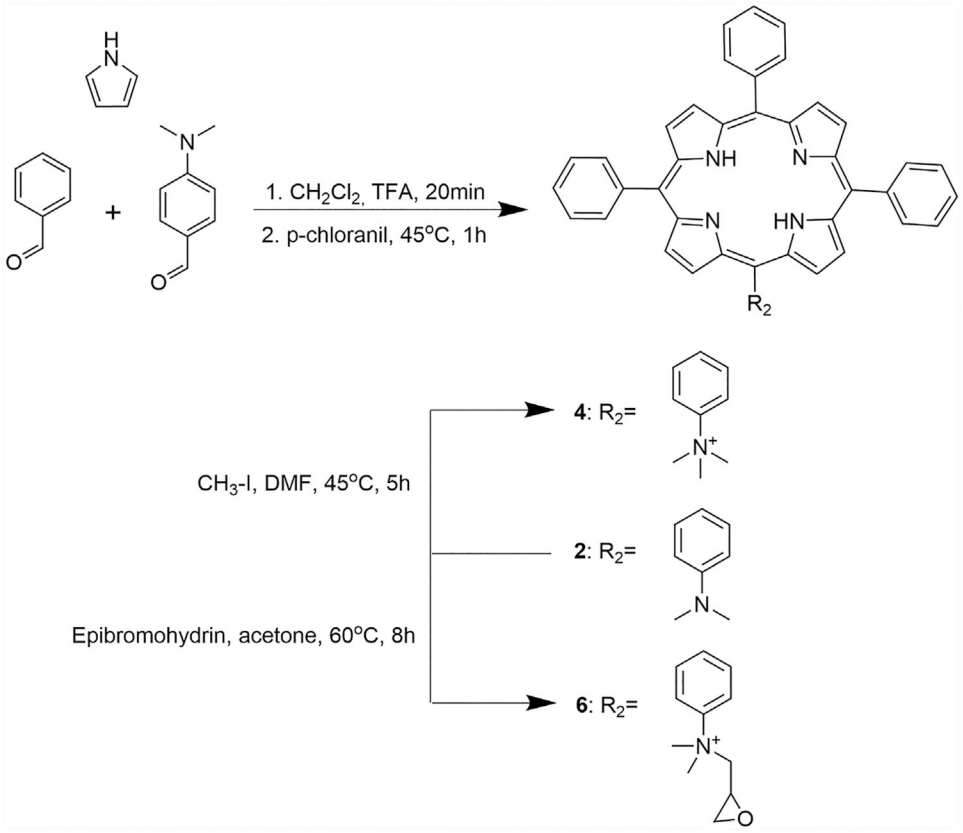


**Scheme 2.**
Synthesis of porphyrins 2, 4, and 6.

**TABLE 1.**

Major (+++) and Minor (+) Subcellular Sites of Localization of Cationic Porphyrins in HEp2 Cells

| Compound | ER | Golgi | Mitochondria | Lysosomes |
|---|---|---|---|---|
| **3** | + + + | + + + | − | + + + |
| **4** | + + + | + + + | + | + + |
| **5** | + + + | + + + | − | + + + |
| **6** | + + | + | + | + + + |

**TABLE 2.**

Cytotoxicity (Cell Titer Blue Assay, 1.5 J/cm$^2$), Comparative Singlet Oxygen *Quantum* Yields (Relative to Methylene Blue), and Cellular Uptake at Selected Times of Porphyrins 1–6 in Human HEp2 Cells

| Compound | Dark Cytotoxicity ($LD_{50}$ μM) | Phototoxicity ($LD_{50}$ μM) | Φ | Uptake at 2 h ($10^{-3}$pM/cell) | Uptake at 4 h (pM/cell) | Uptake at 8 h (pM/cell) | Uptake at 24 h (pM/cell) |
|---|---|---|---|---|---|---|---|
| **1** | >200 | >100 | 0.20 | 0.080 ± 0.002 | 0.134 ± 0.007 | 0.210 ± 0.011 | 0.518 ± 0.011 |
| **2** | >200 | >100 | 0.20 | 0.326 ± 0.035 | 0.710 ± 0.027 | 0.901 ± 0.053 | 1.170 ± 0.013 |
| **3** | >200 | 7.4 | 0.61 | 3.10 ± 0.052 | 4.43 ± 0.093 | 5.45 ± 0.088 | 5.45 ± 0.076 |
| **4** | >200 | 2.4 | 0.52 | 3.90 ± 0.024 | 5.29 ± 0.085 | 5.36 ± 0.072 | 5.40 ± 0.330 |
| **5** | >200 | 100 | 0.59 | 0.142 ± 0.091 | 0.322 ± 0.012 | 0.403 ± 0.018 | 0.778 ± 0.023 |
| **6** | >200 | 38 | 0.35 | 0.142 ± 0.016 | 0.252 ± 0.002 | 0.429 ± 0.004 | 1.06 ± 0.038 |